

# Geochronology and geochemistry of high-pressure granulites of the Arthur River Complex, Fiordland, New Zealand: Cretaceous magmatism and metamorphism on the palaeo-Pacific Margin

J. A. HOLLIS,<sup>1,\*</sup> G. L. CLARKE,<sup>1</sup> K. A. KLEPEIS,<sup>2</sup> N. R. DACZKO<sup>1,†</sup> AND T. R. IRELAND<sup>3</sup>

<sup>1</sup>School of Geosciences, University of Sydney, NSW 2006 Australia (Julie.Hollis@ansto.gov.au)

<sup>2</sup>Department of Geology, The University of Vermont, Burlington, VT 05405 USA

<sup>3</sup>Research School of Earth Sciences, Australian National University, Canberra ACT 0200 Australia

**ABSTRACT** The Arthur River Complex is a suite of gabbroic to dioritic orthogneisses in northern Fiordland, New Zealand. The Arthur River Complex separates rocks of the Median Tectonic Zone, a Mesozoic island arc complex, from Palaeozoic rocks of the palaeo-Pacific Gondwana margin, and is itself intruded by the Western Fiordland Orthogneiss. New SHRIMP U/Pb single zircon data are presented for magmatic, metamorphic and deformation events in the Arthur River Complex and adjacent rocks from northern Fiordland. The Arthur River Complex orthogneisses and dykes are dominated by magmatic zircon dated at 136–129 Ma. A dioritic orthogneiss that occurs along the eastern margin of the Complex is dated at  $154.4 \pm 3.6$  Ma and predates adjacent plutons of the Median Tectonic Zone. Rims on zircon cores from this sample record a thermal event at *c.* 120 Ma, attributed to the emplacement of the Western Fiordland Orthogneiss. Migmatitic Palaeozoic orthogneiss from the Arthur River Complex ( $346 \pm 6$  Ma) is interpreted as deformed wall rock. Very fine rims ( $5\text{--}20 \mu\text{m}$ ) also indicate a metamorphic age of *c.* 120–110 Ma. A post-tectonic pegmatite ( $81.8 \pm 1.8$  Ma) may be related to phases of crustal extension associated with the opening of the Tasman Sea. The Arthur River Complex is interpreted as a batholith, emplaced at mid-crustal levels and then buried to deep crustal levels due to convergence of the Median Tectonic Zone arc and the continental margin.

**Key words:** Arthur River Complex; Fiordland; geochronology; Median Tectonic Zone; Western Fiordland Orthogneiss.

## INTRODUCTION

Plutons and high-grade orthogneisses in Fiordland and Westland, New Zealand record a Mesozoic history of island arc magmatism, arc-continent collision and extensional magmatism culminating in the opening of the Tasman Sea. During the Mesozoic, rocks of the Western Province of New Zealand constituted the Gondwana margin with several outboard terranes comprising the Eastern Province and Median Tectonic Zone (MTZ). Plate tectonic reconstructions indicate that this was a period of rapid change in tectonism over a wide area. From the geological record it has been difficult to obtain definitive constraints on the tectonic processes that operated. For instance, the Western Fiordland Orthogneiss (WFO) constitutes a major part of the Western Province in Fiordland and consists of granulite facies orthogneisses emplaced in the Early Cretaceous from 126 to 116 Ma through to as young as 108 Ma (Mattinson *et al.*, 1986; Gibson

*et al.*, 1988; Gibson & Ireland, 1995). The WFO and its upper crustal equivalent, the Separation Point Suite, have been variably interpreted as the products of all three of the elements listed above, *viz.* island arc magmatism, arc-continent collision, and extensional magmatism (Mattinson *et al.*, 1986; Gibson *et al.*, 1988; Bradshaw, 1989a, 1990; Muir *et al.*, 1995; Brown, 1996; Clarke *et al.*, 2000; Daczko *et al.*, 2001a,b).

The Median Tectonic Zone (MTZ) plays an important role in tectonic reconstructions because it was immediately outboard of the palaeo-Gondwana margin and itself appears to be a complicated assemblage of Palaeozoic to Mesozoic plutonic rocks. Previous geochronological examinations of the rocks of the MTZ indicate two distinct phases of magmatic activity, at 345–226 Ma and 168–137 Ma (Muir *et al.*, 1998). There is a discrete break in age between the youngest MTZ rocks of the Darran Complex (137 Ma) and the oldest rocks of the WFO (126 Ma). As such, the WFO and MTZ rocks have been treated as distinct units with different histories. In Northern Fiordland the WFO shows intrusive relationships with rocks of the Arthur River Complex (ARC). In this region there is a firm constraint on the nature of the crust into which the WFO was emplaced.

\* Present address: Materials and Engineering Science, ANSTO, PMBI, Menai, NSW 2234, Australia.

† Present address: Jackson School of Geosciences, The University of Texas at Austin, Austin, TX 78712, USA.

The ARC is a composite body consisting of gabbroic to dioritic gneisses that lies geographically between the Darran Complex and the WFO. On the basis of their similar geochemistries Blattner (1991) proposed that the ARC and Darran Complex may represent the same rocks that were variably deformed and metamorphosed across a westward-increasing strain gradient. In their SHRIMP zircon U–Pb geochronology of Harrison Gneiss from the ARC at Milford Sound, Tulloch *et al.* (2000) found zircon with Palaeozoic (*c.* 360 Ma) and Cretaceous (*c.* 134 Ma) cores, both with *c.* 120 Ma metamorphic rims. This was interpreted as either a Palaeozoic rock with Cretaceous metamorphic overprints, one of which corresponds to the emplacement of the WFO at *c.* 120 Ma, or a Cretaceous rock (*c.* 134 Ma) with Palaeozoic inheritance and a later Cretaceous metamorphic overprint. Tulloch *et al.* (2000) preferred the former interpretation but they also indicated the difficulties associated with the geological interpretation of the data from a single unit in a metamorphic complex. Nevertheless, the age and inheritance of the Harrison Gneiss is distinct from the characteristics of the Darran Complex, and these data suggest that the ARC is a key element in the interpretation of the emplacement of the WFO and thence the Cretaceous tectonic history of New Zealand.

In this paper we address the transition of the Fiordland region from arc magmatism to arc-continent collision by examining the timing of emplacement, metamorphism and deformation, and the geochemistry of the ARC with respect to the MTZ and WFO. These issues are addressed using U–Pb single zircon geochronology of widely spaced samples and a comparative study of the major and trace element geochemistry of the samples.

## GEOLOGICAL AND GEOCHRONOLOGICAL SETTING

### Regional setting

The South Island of New Zealand has been subdivided into three regimes (Fig. 1; Landis & Coombs, 1967; Bishop *et al.*, 1985); the Eastern Province, the Western Province, and between them the Median Tectonic Zone (MTZ; Kimbrough *et al.* 1993, 1994) or Median Batholith (Mortimer *et al.*, 1999).

The Eastern Province comprises fault-bound Permian to early Cretaceous arc volcanic rocks, arc-derived sedimentary rocks and accretionary complexes. The bulk of the Eastern Province comprises sedimentary rocks of the Torlesse Supergroup and Caples Group, and associated Haast Schist metamorphic rocks. In the south and west of the Eastern Province is a sequence of Permo-Triassic, predominantly volcanoclastic, rocks including Maitai, Murihiku and Brook St Terranes (Kimbrough *et al.*, 1992).

To the west, the MTZ consists of a series of subduction-related I-type plutonic, volcanic and

sedimentary rocks thought to have formed in a Mesozoic magmatic arc outboard of the Gondwana margin, active from 345 to 226 Ma and again from 168 to 137 Ma (Bradshaw, 1993; Kimbrough *et al.*, 1993, 1994; Muir *et al.*, 1998). Devonian-Carboniferous granites occur apparently as basement in the MTZ but it remains unclear as to whether these are an essential element of the MTZ or related to penecontemporaneous intrusions in the Western Province. In both the Nelson/Westland and Fiordland regions plutons belonging to the volumetrically dominant Late Jurassic to early Cretaceous plutons tend to lie within the western part of the MTZ (Kimbrough *et al.*, 1994).

Contacts between the Eastern Province and the MTZ are largely fault controlled and the timing of amalgamation remains unclear. However, on the basis of an interpreted intrusive relationship with the Brook Street Terrane (Williams & Harper, 1978), the MTZ and the Eastern Province may have been amalgamated by the Late Triassic. By at least *c.* 126 Ma (Muir *et al.*, 1995; Kimbrough *et al.*, 1994) these two terranes had accreted onto the Western Province, which is thought to represent the rifted and tectonically disrupted fragments of the Triassic to early Cretaceous palaeo-Pacific Gondwana margin.

The formerly contiguous upper crustal Nelson/Westland and lower crustal Fiordland regions of the Western Province were displaced by 500 km of Tertiary dextral slip along the Alpine Fault (Fig. 1). In the Nelson/Westland region, the Western Province consists of low grade metasedimentary rocks punctuated by two generations of granites of Carboniferous-Devonian age and of Cretaceous age, the largest of which are the Karamea batholith (*c.* 375 Ma; Muir *et al.* 1996) and the Separation Point Suite (118–111 Ma; Harrison & McDougall, 1980; Kimbrough *et al.*, 1993, 1994; Muir *et al.*, 1994). Palaeozoic and Cretaceous metamorphic rocks to upper amphibolite facies are derived from the sedimentary and intrusive rocks (White, 1994; Ireland, 1992a; Kimbrough & Tulloch, 1989).

In Fiordland, exposure of the Western Province is at a much deeper crustal level and includes amphibolite to granulite facies Palaeozoic and Mesozoic orthogneisses and metasedimentary rocks. On the basis of detrital zircon populations, sedimentary protoliths to the majority of the metasedimentary rocks of the Western Province in Fiordland are thought to have been deposited between 500 and 440 Ma (Ireland, 1992b; Ireland & Gibson, 1998). These zircon populations indicate that the rocks are equivalent to the extensive Ordovician turbidites of south-eastern Australia, being indicative of a similar source in these probably contiguous regions that formed the Pacific margin of Gondwana (e.g. Cooper & Tulloch, 1992; Gibson, 1992; Ireland, 1992b; Pankhurst *et al.*, 1993; Muir *et al.*, 1994, 1996; Wysoczanski *et al.*, 1997; Ireland & Gibson, 1998; Mukasa & Dalziel, 2000).

In the mid-Palaeozoic, the Western Province experienced the first of two major magmatic/

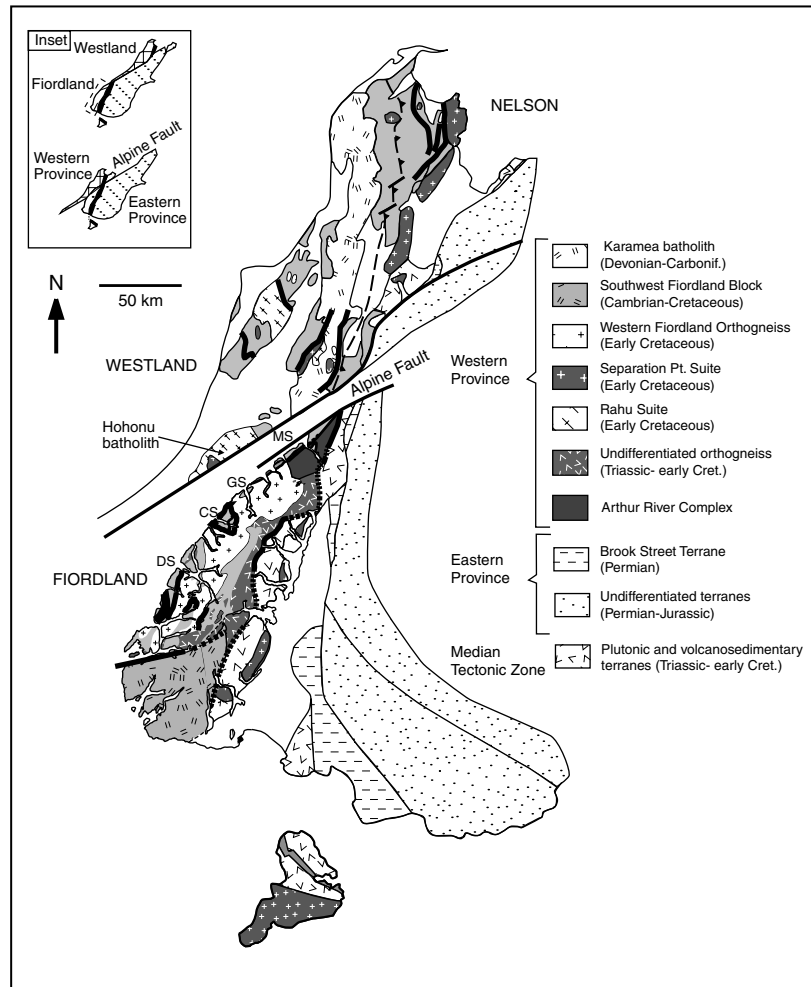


**Fig. 1.** Pre-late Cenozoic reconstruction of Western New Zealand (after Klepeis *et al.*, 2003). MS is Milford Sound, GS is George Sound, CS is Caswell Sound, DS is Doubtful Sound.

metamorphic events, the *c.* 380–330 Ma Tuhua Orogeny. Between *c.* 380–360 Ma significant calc-alkaline plutonism occurred in the Western Province of New Zealand, south-east Australia, and West Antarctica (Fig. 2). In the Western Province, magmatism resulted in the emplacement of numerous plutons in Fiordland and the voluminous Karamea Batholith in Westland (Muir *et al.*, 1994, 1996; Ireland & Gibson, 1998; Gibson & Ireland, 1999). This is thought to have been responsible for the high-*T*, low-*P* metamorphism of metasedimentary rocks in Fiordland and Westland at *c.* 360 Ma (M1; Gibson *et al.*, 1988; Gibson, 1992; Ireland & Gibson, 1998). It was followed by high-*P* metamorphism in Fiordland at *c.* 330 Ma (M2; Ireland & Gibson, 1998). On the basis of the geochemistry of the mid-Palaeozoic plutons and the metamorphic history, the Tuhua Orogeny is thought to reflect subduction-related magmatism and metamorphism along the palaeo-Pacific Gondwana margin.

In the early Cretaceous the WFO, a large composite batholith of metadiorites and metagabbros, intruded the Palaeozoic Tuhua Sequence in Fiordland. On the basis of similar geochemistry and timing of

emplacement, the WFO is thought to be the lower-crustal equivalent of the SPS (Harrison & McDougall, 1980; Kimbrough *et al.*, 1993, 1994; Muir *et al.*, 1994, 1995). Emplacement of the WFO between 126 and 119 Ma (Mattinson *et al.*, 1986; McCulloch *et al.*, 1987; Gibson *et al.*, 1988; Gibson & Ireland, 1995) was followed by hydrous retrogression and cooling to < 300–400 °C by *c.* 90 Ma (Rb-Sr biotite age, Aronson, 1968; Mattinson *et al.*, 1986; K-Ar hornblende age, Gibson *et al.*, 1988). The WFO has been regarded by a number of authors as the heat source for regional high-grade metamorphism of Western Province rocks in Fiordland at 650–700 °C and 12–13 kbar (e.g. Bradshaw, 1985, 1989a, 1990, 1991; Mattinson *et al.*, 1986; McCulloch *et al.*, 1987). However, dominantly Palaeozoic <sup>40</sup>Ar–<sup>39</sup>Ar and <sup>40</sup>K–<sup>40</sup>Ar ages recorded by orthogneisses and metasedimentary rocks in central and southern Fiordland (Gibson *et al.*, 1988) suggest that the thermal effect of the WFO is not of regional significance, the Palaeozoic Tuhua Orogeny being responsible for the generation of regional metamorphic assemblages in metasedimentary gneisses (M1 and M2 of Ireland & Gibson, 1998).

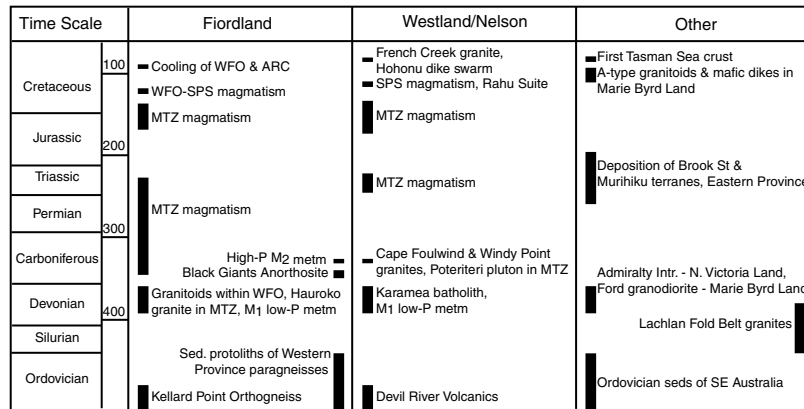


**Fig. 2.** Summary of the geochronology of Western New Zealand and related regions. (Data from Adams, 1987; Aronson, 1968; Borg *et al.*, 1987; J.D. Bradshaw (1989); J.Y. Bradshaw, 1991; Gibson & Ireland, 1995, 1998; Ireland, 1992b; Ireland & Gibson, 1998; Kimbrough *et al.*, 1993, 1994; Luyendyk, 1995; McCulloch *et al.*, 1987; Mattinson *et al.*, 1986; Muenker & Cooper, 1995; Muir *et al.*, 1994, 1995, 1996, 1998; Tulloch *et al.*, 1991; Waight *et al.*, 1997; Weaver *et al.*, 1991; Weissel & Hayes, 1977; Williams *et al.*, 1992).

### Arthur River Complex

The ARC, which covers a large area of northern Fiordland, is a composite body of largely garnet-hornblende-bearing homogeneous mafic gabbroic gneiss termed the Milford Gneiss, banded dioritic gneiss termed the Harrison Gneiss, and lesser migmatite and ultramafic rock (Figs 1 & 3; Wood, 1972; Blattner, 1991). Two-pyroxene-hornblende-bearing gabbroic and dioritic gneisses, known as the Pembroke Granulite, form a low-strain zone within the Milford Gneiss and illustrate the early structural and metamorphic history of the ARC, discussed below. The ARC is intruded to the south by the WFO. To the east it is bounded by the *c.* 143–137 Ma gabbroic to dioritic Darran Complex of the MTZ (Mattinson *et al.*, 1986; Kimbrough *et al.*, 1994; Muir *et al.*, 1998; Wandres *et al.*, 1998; Nathan *et al.*, 2000) and the dioritic to tonalitic Indecision Creek Complex (Bradshaw, 1985) along what is interpreted as a gradational (Bradshaw, 1990) and/or faulted (Blattner, 1978, 1991; Tulloch *et al.*, 2000) contact. The ARC has been considered to be genetically linked with Palaeozoic orthogneisses of the Western Province (Bradshaw, 1990), however, the uncertain nature of this boundary and geochemical similarities between the ARC and the Darran Complex have led to suggestions that the ARC may represent a deformed equivalent of the Darran Complex (Blattner, 1991).

To the west, the ARC is bound by mylonites and cataclasites of the Anita Shear Zone, interpreted as a major lower crustal shear zone formed during incipient rifting of the Gondwana margin and the opening of the Tasman Sea in the mid-Cretaceous (Klepeis *et al.*, 1999). The Anita Shear Zone juxtaposes the ARC with Palaeozoic orthogneisses and metasedimentary rocks correlated with the Tuhua Sequence.

The TIMS and SHRIMP U-Pb zircon study of Tulloch *et al.* (2000) represents the only geochronological study of the ARC. Tulloch *et al.* (2000) analysed zircon from a sample of the Milford Gneiss from

the north wall of Milford Sound, identifying Palaeozoic (*c.* 360 Ma) and Cretaceous (*c.* 134 Ma) cores, both with *c.* 120 Ma rims. On this basis they suggested the Milford Gneiss was emplaced in the Palaeozoic and experienced two thermal events in the Cretaceous. K-Ar hornblende and plagioclase ages from the Milford and Harrison Gneisses are consistent with appreciable cooling of the ARC by *c.* 110–90 Ma (Nathan *et al.*, 2000), consistent with similar cooling ages from the WFO (Gibson *et al.*, 1988).

The ARC experienced at least four deformational/metamorphic events, covered in detail in Clarke *et al.* (2000) and Daczko *et al.* (2001a) and outlined briefly here. Within the Pembroke Granulite two-pyroxene S1 assemblages reflect conditions of < 8 kbar and > 750 °C, only patchily recrystallized during later deformation. A lattice pattern of D2 fractures are interpreted as having formed via strain partitioning in the lower crust (Daczko *et al.*, 2001a). D2 fractures are filled with trondhjemitic veins, which served as the loci for garnet reaction zones. These alteration zones, in which hornblende has been statically pseudomorphed by fine-grained garnet and clinopyroxene, can also be found in the WFO (Blattner, 1976; Oliver, 1977; Bradshaw, 1989b, 1990), constraining their formation to the early Cretaceous, and formed at conditions of approximately 14 kbar and 750–850 °C (Clarke *et al.*, 2000; Daczko *et al.*, 2001b). In the ARC, garnet reaction zones are variably deformed by steeply north and south dipping D3 and gently south-east dipping D4 mylonitic shear zones, both formed under conditions of approximately 14 kbar and 680 °C (Clarke *et al.*, 2000; Daczko *et al.*, 2001a). D4 was also responsible for the formation of ductile thrusts in the Pembroke Granulite (Daczko *et al.*, 2001a), shear zones in the WFO in Poison Bay (Clarke *et al.*, 2000), and the main fabric-forming gneissosity in the Milford and Harrison Gneisses of the ARC.

The formation of high-*P* garnet reaction zones in the ARC and WFO, postdating lower-pressure assemblages, indicate burial from < 8 kbar to *c.* 14 kbar

during granulite facies metamorphism in the early Cretaceous (Bradshaw, 1985, 1989a, 1990; Clarke *et al.*, 2000; Daczko *et al.*, 2001a,b). Coupled with structural evidence for deep crustal thrust belts within the ARC (D4), oblique transpressional movement associated with garnet reaction zone formation (Daczko *et al.*, 2001a), and calc-alkaline geochemical signatures of MTZ and WFO rocks (McCulloch *et al.*, 1987; Blattner, 1991; Muir *et al.*, 1995, 1998; Wandres *et al.*, 1998), there exists strong support for oblique convergence in a subduction-related arc setting in the early Cretaceous. Muir *et al.* (1995, 1998) proposed that this relates to the convergence of the MTZ arc with the Gondwana margin, resulting in partial melting of the subducted arc producing WFO-SPS magmatism.

## SAMPLE DESCRIPTIONS

Five samples of orthogneisses and a sample of a syn-post-D4 dyke were collected from widely spaced locations to constrain emplacement, metamorphism and deformation of the ARC. Orthogneisses included two homogeneous gabbroic and dioritic orthogneisses from the north wall of Milford Sound (9628 A, 9605), a migmatitic gneiss from Camp Oven Creek (CO3), and weakly deformed dioritic gneisses from Mt Edgar in the Franklin Mountains (ME1) and from Steep Hill, approximately 3 km east of Mt Danger (0224c; Fig. 3). A sample of a syn-post-D4 felsic dyke was collected from Devil's Armchair, approximately 5 km south of Mitre Peak (02DA; Fig. 3). A post-D4 pegmatite sample from the Pembroke Valley above Milford Sound (PB3) was collected to place a minimum constraint on D4 deformation in the Milford Gneiss. To constrain the eastern limit of the ARC with the Darran Complex a sample of a dioritic banded orthogneiss was collected from Selwyn Creek (SC2; Fig. 3). Sample locations are shown in Fig. 3. The petrography of these samples is listed in Table 1.

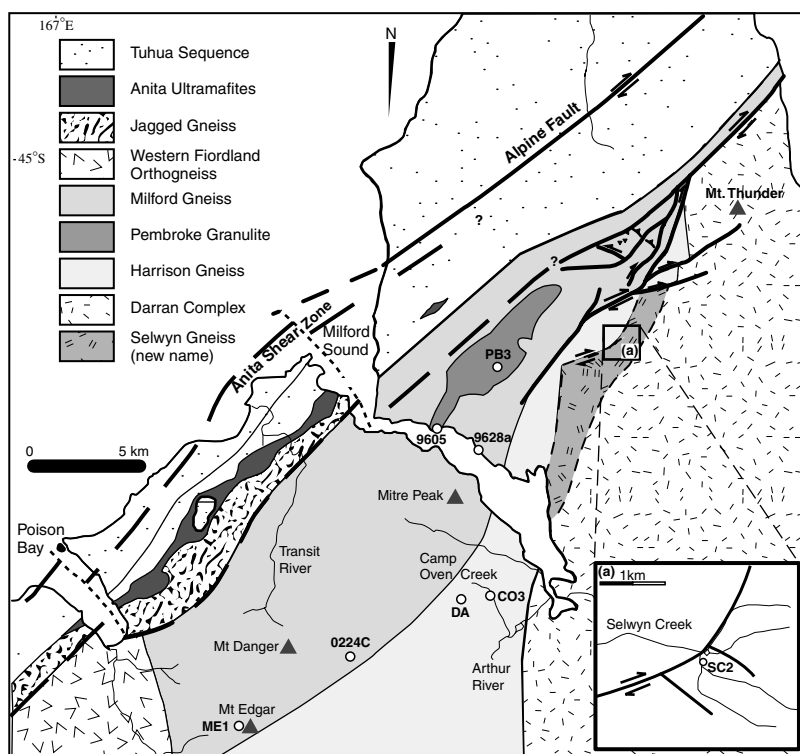


**Fig. 3.** Geology of northern Fiordland at Milford Sound showing locations of samples. (a) Smaller scale insert of the location of sample SC2.

**Table 1.** Sample localities and petrography. Abbreviations follow the scheme of Kretz (1983). Additional abbreviations are as follows: phg mi is phengitic white mica.

Sample	Location	Assemblage	Deformation/textural features
9605	Milford Sound (north wall)	Gr <sub>t</sub> -hbl-czo-pl-qtz-rt, late bt-phg mi	Strong S: aligned hbl-czo
9628 A	Milford Sound (north wall)	Gr <sub>t</sub> -hbl-czo-bt-pl-qtz-rt, late ep-chl	Weak S4: aligned hbl-czo
CO3	Camp Oven Crk	Gr <sub>t</sub> -czo-bt-pl-qtz-rt, late phg mi	Moderate S4: aligned bt and syn-D4 felsic segregations interpreted as incipient melt textures
ME1	Mt Edgar	Gr <sub>t</sub> -hbl-czo-bt-pl-qtz-rt	Weak S1: aligned hbl-czo-bt
02DA	Devil's Armchair	Pl-qtz, minor czo-bt-phg mi, ± grt	Granoblastic. Dyke cuts D4 in Camp Oven Creek metadiorites
0224C	Steep Hill	Hbl-czo-ep-white mi-pl-qtz-rt-ap ± garnet, late hbl-bt	Granoblastic. Dyke cuts layered mafic gneisses
PB3	Pembroke Valley	Pl-qtz-ms	Granoblastic. Pegmatite cuts S4 in Milford Gneiss.
SC2	Selwyn Crk	Gr <sub>t</sub> -hbl-czo-pl-phg mi-qtz-rt-ap	Moderate S4: aligned hbl. Syn-D4 felsic veins with peritectic grt

## ANALYTICAL TECHNIQUES

Samples were crushed and separated using heavy liquids at the CSIRO Materials Division at North Ryde, Sydney. Individual zircon were hand picked from separates, mounted in epoxy along with SHRIMP zircon standard material, and polished until exposed through their mid-sections. Cathodoluminescence (CL) imaging was carried out on a Hitachi S-2250 N SEM at the Australian National University (ANU) Electron Microscopy Unit and a JEOL 35C SEM with attached Oxford Instruments MonoCL imaging and spectral analysis system at the University of Technology, Sydney. CL imaging was used to reveal the internal structures of the zircon for the purpose of interpreting zircon growth and metamorphic histories and choosing appropriate sites for SHRIMP analyses. Representative CL images of zircon from ARC gneisses are shown in Fig. 4. Back-scattered electron imaging was carried out on a Cambridge S360 SEM at the ANU Electron Microscopy Unit and a Philips SEM505 at the Key Centre for Electron Microscopy at the University of Sydney. This was designed to reveal any structures not apparent in the CL images, and to show included phases and surface features for the purpose of choosing appropriate sites for SHRIMP analyses. Some rims on zircon cores identified from CL imaging were too small for analysis. In order to analyse these, the zircon were remounted in epoxy and lightly polished so that the rims were just visible on the surface of the mount. Analyses were carried out by depth profiling through the grain surfaces such that the ion beam penetrated normal rather than parallel to the rims, giving a broader area of rim material and reducing the risk of mixed core-rim analyses.

U-Pb-Th isotopic data were collected on SHRIMP I (Sensitive High Resolution Ion MicroProbe) and SHRIMP RG at the ANU using standard operating procedures (Muir *et al.*, 1996). A 3–5 nA primary  $O_2^-$  ion beam is focused into a 30- $\mu$ m diameter spot that sputters material from the sample to form a flat-bottomed crater. Positive ions sputtered from the crater are extracted and are mass separated into the peaks of interest:  $^{90}Zr^{16}O$ ,  $^{204}Pb$ ,  $^{206}Pb$ ,  $^{207}Pb$ ,  $^{208}Pb$ ,  $^{238}U$ ,  $^{232}Th^{16}O$ , and  $^{238}U^{16}O$ . U-Pb ratios were normalised to UO/U and calibrated to 417 Ma zircon from the Temora granite, NSW (Black *et al.*, 2003). Uncertainty in the measurement of U-Pb is a function of the internal measurement uncertainties,

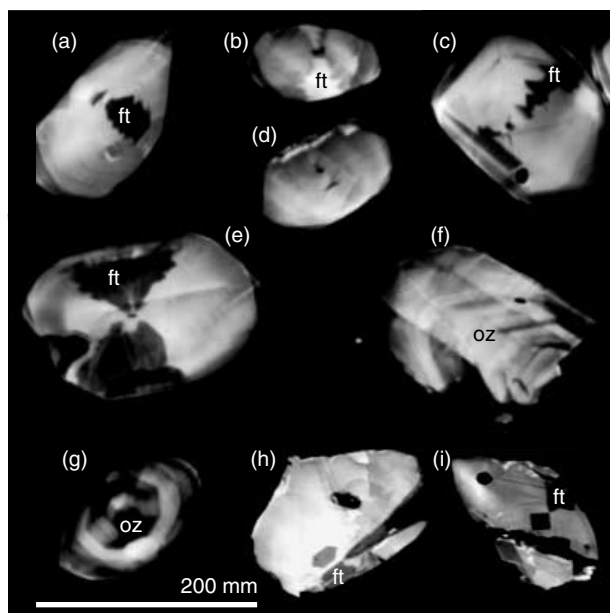


**Fig. 4.** Cathodoluminescence (CL) images of representative zircon morphologies from the ARC (sample ME1 and 0224C). Ft is fir-tree zonation and oz is oscillatory zonation.

often dominated by counting statistics, and of the external reproducibility of the standard materials. In this case, the uncertainties are largely dominated by the counting statistics of the individual measurement of the Temora standard. The final error in the mean of the standards was propagated through to the uncertainty on the final sample age.

The uncorrected Pb data for all samples are presented in the form of Tera-Wasserberg concordia diagrams, on which measured ratios are plotted with respect to the  $^{207}Pb/^{206}Pb$ - $^{238}U/^{206}Pb$  concordia. In the case of Phanerozoic zircon  $^{238}U/^{206}Pb$  ages are regarded as more reliable than  $^{235}U/^{207}Pb$  or  $^{207}Pb/^{206}Pb$  ages because of the low proportion of  $^{235}U$  available for incorporation into young zircon, resulting in only small proportions of radiogenic  $^{207}Pb$ . Using the  $^{204}Pb/^{206}Pb$  common lead correction, the low count rates from  $^{204}Pb$  and  $^{207}Pb$  result in poor counting statistics and therefore result in significant error propagation into  $^{207}Pb/^{206}Pb$  age calculations for young zircon. In this study the  $^{207}Pb/^{206}Pb$  ratio was used to monitor common Pb ( $^{207}Pb/^{206}Pb$  correction method of Muir *et al.*, 1996). Each datum is assumed to be a simple mixture of common and radiogenic Pb. Thus  $^{238}U/^{206}Pb$  ages can be calculated by extrapolating from the common Pb value through the measured datum onto concordia. Individual ages from each analysis are given with one-standard deviation uncertainty; final ages for each sample are reported with two-standard deviation uncertainty on the weighted mean. Probability diagrams are also presented for samples in which multiple zircon age populations exist. The illustrated curve in each represents the summation of unit-area gaussian curves for all data from a sample.

Major and trace element bulk-rock analyses of samples of the ARC and WFO were obtained using a Philips PW2400 X-ray fluorescence (XRF) spectrometer at the University of New South Wales and by neutron activation analysis (NAA) using the HIFAR reactor at the Lucas Heights Science and Technology Centre. Samples analysed using XRF spectrometry were crushed to a fine powder, dried, and then either fused into 40 mm glass discs for major element analysis or pressed into powder briquettes set in a backing of boric acid for trace element analysis. Full details of sample preparation and analysis method are given in Norrish & Hutton (1969). Samples analysed via NAA were weighed and heat-sealed in polypropylene vials and activated for 10–30 min, along with an attached flux monitor, in a thermal neutron flux of  $2-4 \times 10^{12} \text{ cm}^{-2} \text{ s}^{-1}$ . The resulting gamma spectrum for each sample and monitor was measured simultaneously after 7 days to normalise and adjust for dead-time correlations. The gamma ray spectra were then measured using hyperpure Ge coaxial detectors and converted into concentrations using the Becquerel Laboratories' in-house programs.

## U-PB ZIRCON SHRIMP RESULTS

U and Th concentrations and ratios,  $^{204}Pb/^{206}Pb$ ,  $^{207}Pb/^{206}Pb$ , and  $^{238}U/^{206}Pb$  ratios, and age data for each analysis are given in Table S1 available from <http://www.blackwellpublishing.com/products/journals/suppmat/JMG/JMG443/JMG443sm.htm>. Graphical representations of the uncorrected data are presented in Fig. 5.

### Arthur River Complex

#### Milford Gneiss, Milford Sound (9605, 9628 A)

Zircon specimen 9605 are typically blocky and show a weak dull CL response. Eight analyses give a  $^{238}U/^{206}Pb$  age of  $131.3 \pm 2.9 \text{ Ma}$  ( $2 \sigma$ , MSWD 1.66; Fig. 5a). Th/U ratios range from 0.40 to 0.54. Zircon is more common in sample 9628 A and is morphologically very similar to those of 9605. They are generally

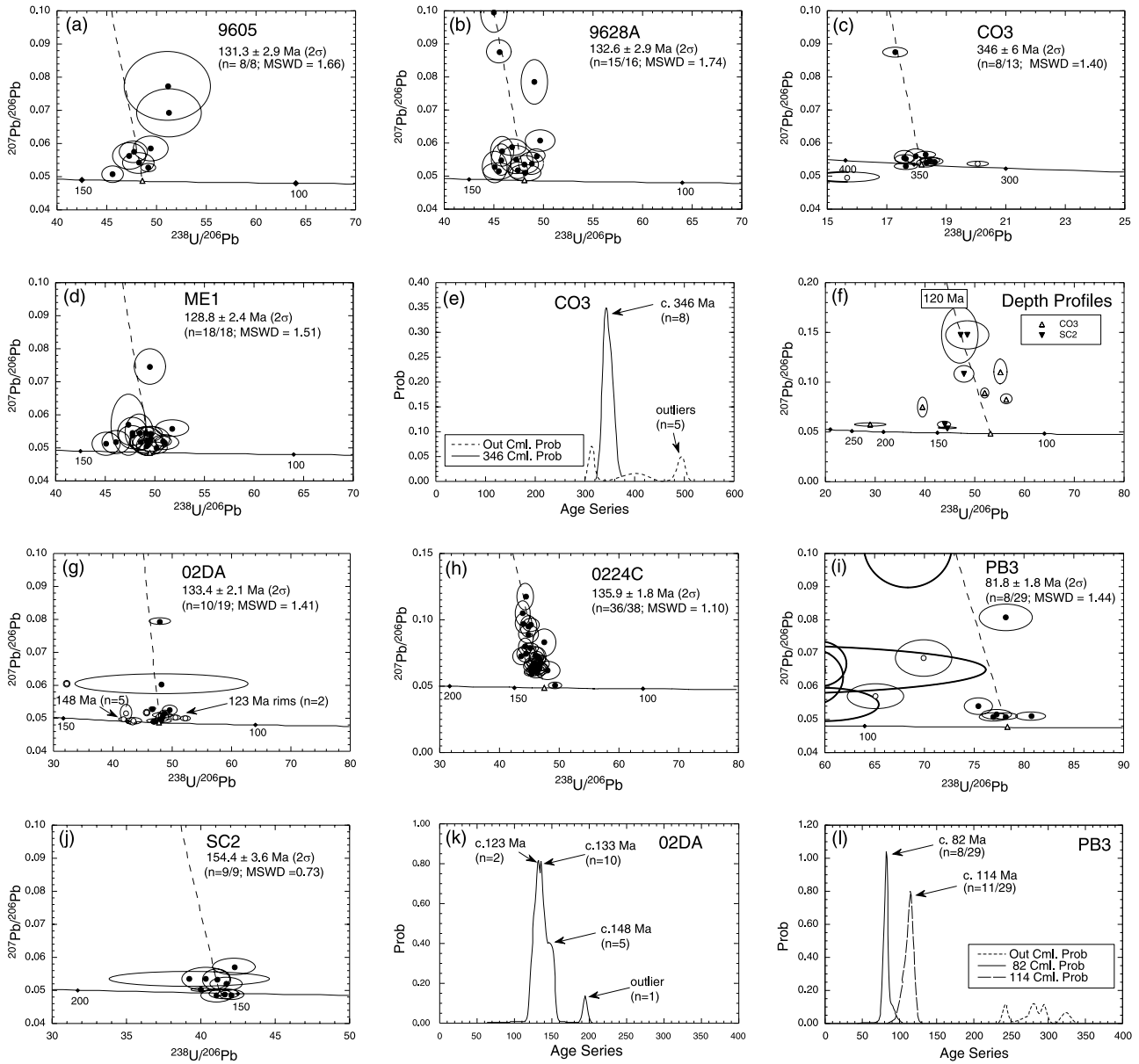


**Fig. 5.** Tera-Wasserberg plots of SHRIMP zircon data from (a) 9605 (b) 9628 A (c) CO3 cores (d) ME1 (f) depth profiles of grain surfaces (rims) of CO3 and SC2 (g) O2DA (h) O224C (i) PB3, and (j) SC2 cores, and probability plots of age populations from (e) CO3 (k) O2DA, and (l) PB3.

ellipsoid and rounded, with a patchy CL response. Some show development of growth sectors with zig-zag edges, known as fir-tree zonation (Raven & Dickson, 1989; Vavra *et al.*, 1996). Fifteen of 16 zircon analysed give a  $^{238}\text{U}/^{206}\text{Pb}$  age of  $132.6 \pm 2.8$  Ma ( $2\sigma$ , MSWD 1.74; Fig. 5b) with an outlier at  $121.3 \pm 4.1$  Ma. Th/U ratios range from 0.37 to 0.99.

*Migmatitic gneiss, Camp Oven Creek (CO3)*

Eight of 13 oscillatory-zoned grains analysed give a  $^{238}\text{U}/^{206}\text{Pb}$  age of  $346 \pm 6$  Ma ( $2\sigma$ , MSWD 1.40;

Fig. 5c; Table 1). A few older ages, *c.* 1073–400 Ma, reflect inherited zircon probably from a sedimentary protolith. Also, a younger age ( $313.2 \pm 5.4$  Ma) is interpreted as a mixed analysis from an oscillatory-zoned core and thin bright rim that proved too small to analyse (Fig. 5e). Th/U ratios range from 0.18 to 1.41. Depth profiling of the thin rims identified *c.* 120–110 Ma Cretaceous  $^{238}\text{U}/^{206}\text{Pb}$  ages for three grains:  $109.0 \pm 2.1$  Ma,  $117.5 \pm 1.9$  Ma, and  $108.2 \pm 3.1$  Ma. Th/U ratios range from 0.00 to 0.03. Three other grains gave  $^{238}\text{U}/^{206}\text{Pb}$  ages of  $332.5 \pm 7.0$  Ma,  $156.8 \pm 4.3$  Ma, and  $216.2 \pm 22.8$  Ma (Fig. 5f). These

may represent mixed ages between the Palaeozoic cores and Cretaceous rims, or Pb loss from Palaeozoic rims during Cretaceous metamorphism.

#### *Milford Gneiss, Mt Edgar (ME1)*

All 18 analyses of homogeneous, patchy, and sector zoned grains (Fig. 4a–e) and grains with weak oscillatory zonation (Fig. 4f,g) give a  $^{238}\text{U}/^{206}\text{Pb}$  age of  $128.8 \pm 2.4$  Ma ( $2\sigma$ , MSWD 1.51; Fig. 5d). Th/U ratios range from 0.21 to 1.78.

#### *Felsic dyke, Devil's Armchair (02DA)*

Ten of 17 analyses of oscillatory zoned cores give a  $^{238}\text{U}/^{206}\text{Pb}$  age of  $133.4 \pm 2.1$  Ma ( $2\sigma$ , MSWD 1.41; Fig. 5g), interpreted as the age of emplacement. Five other analyses of oscillatory zoned cores with  $^{238}\text{U}/^{206}\text{Pb}$  ages clustering around *c.* 148 Ma, and an outlier at  $194.6 \pm 3.0$  Ma are thought to reflect inheritance (Fig. 5k). Th/U ratios range from 0.02 to 1.28. Two analyses of thin homogeneous rims on oscillatory zoned cores give ages of  $125.9 \pm 1.8$  Ma (U/Th = 0.23) and  $122.0 \pm 2.0$  Ma (U/Th = 0.01; Fig. 5k).

#### *Dioritic dyke, Steep Hill (0224C)*

Thirty-six of 38 analyses of grains that have largely homogeneous CL responses (Fig. 4h,i) give a  $^{238}\text{U}/^{206}\text{Pb}$  age of  $135.9 \pm 1.8$  Ma ( $2\sigma$ , MSWD 0.73; Fig. 5h). Th/U ratios range from 0.34 to 1.26. Three older  $^{238}\text{U}/^{206}\text{Pb}$  ages of  $304.9 \pm 27.2$  Ma,  $242.2 \pm 11.2$  Ma, and  $301.2 \pm 94.6$  Ma are thought to represent some Palaeozoic inheritance.

#### **Post-D4 pegmatite, Pembroke Valley (PB3)**

A wide range of ages was immediately apparent on analysis of PB3 but the zircon fall into three categories based on their morphologies. Type 1 zircon (approximately 65%) are blocky and show a dull, patchy CL response. Eleven of 14 grains of this type give a  $^{238}\text{U}/^{206}\text{Pb}$  age of  $113.6 \pm 3.2$  Ma ( $2\sigma$ , MSWD 0.83; Fig. 5l). Of the remaining three grains, two give comparatively young ages of  $87.2 \pm 8.7$  Ma and  $97.2 \pm 4.2$  Ma. The other gives a poorly constrained older age of  $123.7 \pm 62.3$  Ma. Th/U ratios range from 0.00 to 1.06.

The five oscillatory-zoned type 2 zircon grains (*c.* 20%) give  $^{238}\text{U}/^{206}\text{Pb}$  core ages of  $242.5 \pm 3.4$ ,  $272.8 \pm 11.3$ ,  $280.9 \pm 4.3$ ,  $294.5 \pm 3.7$ , and  $324.0 \pm 5.9$  Ma, which are interpreted as inherited ages (Fig. 5l). The oldest grain has a comparatively dark rim, which gives a  $^{238}\text{U}/^{206}\text{Pb}$  age of  $123.8 \pm 1.8$  Ma (analysis 9.1, Table S1), interpreted as a metamorphic overgrowth. Th/U ratios range from 0.21 to 0.75.

Type 3 zircon (15%) have a very dark CL response. Eight analyses give a  $^{238}\text{U}/^{206}\text{Pb}$  age of  $81.8 \pm 1.8$  Ma ( $2\sigma$ , MSWD 1.44; Fig. 5i,l). On the basis of very low

Th (0–21 p.p.m.) and high U (28–2222 p.p.m.) contents, typical of pegmatitic zircon, this is interpreted as the age of pegmatite emplacement.

#### **Dioritic gneiss, Selwyn Creek (SC2)**

All 9 oscillatory and sector-zoned cores analysed give a  $^{238}\text{U}/^{206}\text{Pb}$  age of  $154.4 \pm 3.6$  Ma ( $2\sigma$ , MSWD 0.73; Fig. 5j). Th/U ratios range from 0.14 to 0.91. Five grains were analysed via depth profiling to determine the age of thin, bright CL rims. Three gave  $^{238}\text{U}/^{206}\text{Pb}$  ages of  $117.3 \pm 10.1$ ,  $124.5 \pm 5.2$  and  $120.7 \pm 9.1$  Ma with Th/U ratios of 0.01–0.07. The other two grains gave  $^{238}\text{U}/^{206}\text{Pb}$  ages of  $143.6 \pm 4.0$  and  $142.4 \pm 5.9$  Ma with Th/U ratios of 0.18 and 0.23 (Fig. 5f). The latter are thought to represent either core ages with partial Pb-loss or mixed core-rim ages.

#### **Synopsis**

Samples of the Arthur River Complex show distinct zircon morphologies that correlate well with the age data. Four of the samples (9605, 9628 A, ME1, 0224C) have subhedral-anhedral blocky zircon grains with dull, patchy CL responses, rare weak oscillatory zonation and some overprinting fir-tree sector zonation. Examples of the main morphological features are shown in Fig. 4. These four samples record Cretaceous ages in the range 136–129 Ma. One of these samples (0224C) preserves a few older ages attributed to some Palaeozoic inheritance. A syn-post tectonic felsic dyke from Devil's Armchair (02DA) contains euhedral oscillatory zoned zircon that yield a similar Cretaceous age (with some inheritance). Of these five samples with similar Cretaceous ages all but two fall within error: the ages of ME1 ( $128.8 \pm 2.4$  Ma) and 0224C ( $135.9 \pm 1.8$  Ma) are removed by *c.*  $3\sigma$  from the weighted mean of the ages of all five samples,  $133.0 \pm 2.6$  Ma ( $2\sigma$ ). This is consistent with an age range rather than a single age population. Zircon from sample CO3, morphologically similar to those from 02DA, preserve mid-Palaeozoic core ages with some evidence of older inheritance. Thin rims on oscillatory-zoned cores from both samples (02DA, CO3) record younger Cretaceous ages of *c.* 120–110 Ma.

From near the inferred boundary between the ARC and Darran Complex at Milford Sound, sample SC2 has blocky zircon grains with weak oscillatory zonation, overprinting fir tree sector zoning, and thin homogeneous rims. Cores give a Late Jurassic age of  $154.4 \pm 3.6$  Ma. and rims give Cretaceous age of *c.* 120 Ma. Zircon from a post-D4 pegmatite show three distinct zircon morphologies that correlate with the age data. Subhedral equant grains with a dull CL response give an age of  $113.6 \pm 3.2$  Ma. Euhedral grains with well-defined oscillatory zonation give Late Palaeozoic core ages. Elongate grains with very dark CL responses give an age of  $81.8 \pm 1.8$  Ma.

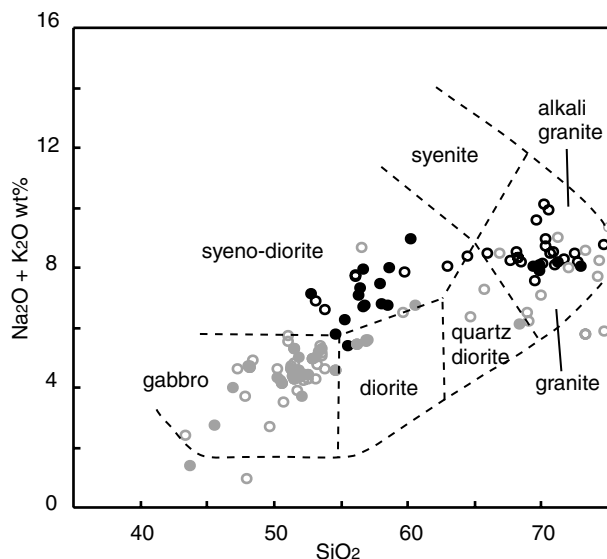


**Fig. 6.** Total alkali-silica plots of the ARC (filled grey circles), MTZ plutons (unfilled grey circles), the WFO (filled black circles), and the SPS (unfilled black circles) using the classification scheme of LeMaitre (1984). Data taken from this study, McCulloch *et al.* (1987), Blattner (1991), Tulloch & Rabone (1993), Muir *et al.* (1994, 1995, 1998), and Wandres *et al.* (1998).

## GEOCHEMISTRY

The geochemistry of the MTZ, WFO and SPS have been covered in considerable detail in the literature (McCulloch *et al.*, 1987; Blattner, 1991; Tulloch & Rabone, 1993; Muir *et al.*, 1994, 1995, 1998; Wandres *et al.*, 1998). Geochemical information on the ARC is more limited (Blattner, 1991). In this section a new geochemical dataset is considered by combining new results from analyses of samples of the ARC and WFO with published data for the WFO, SPS and MTZ plutons. In light of this we assess the relationship between the ARC and other rock suites within the context of the Cretaceous evolution of Western New Zealand.

Rocks of the ARC are dominantly gabbroic, but extend to dioritic and quartz dioritic compositions (Fig. 6).  $\text{SiO}_2$  contents range from *c.* 44–68 wt%, but are generally < 57 wt%. Compositions fall within the calc-alkali field (Fig. 7).  $\text{Na}_2\text{O}$  and  $\text{K}_2\text{O}$  content increases sympathetically with  $\text{SiO}_2$  content, whereas FeO, MgO,  $\text{Al}_2\text{O}_3$  and CaO contents show antithetic trends with respect to  $\text{SiO}_2$  (Fig. 8a–f). The samples show a general trend of light rare earth element (LREE) enrichment and slightly enriched, relatively flat heavy rare earth element (HREE) patterns. Positive K, Sr and Ba anomalies, and negative Nb and Th anomalies are consistent with an island arc calc-alkaline affinity (Fig. 9; e.g. Sun, 1980; Thompson *et al.*, 1984). Selected elemental abundance diagrams incorporating our data and existing published data illustrate the compositional ranges of the ARC, MTZ, WFO

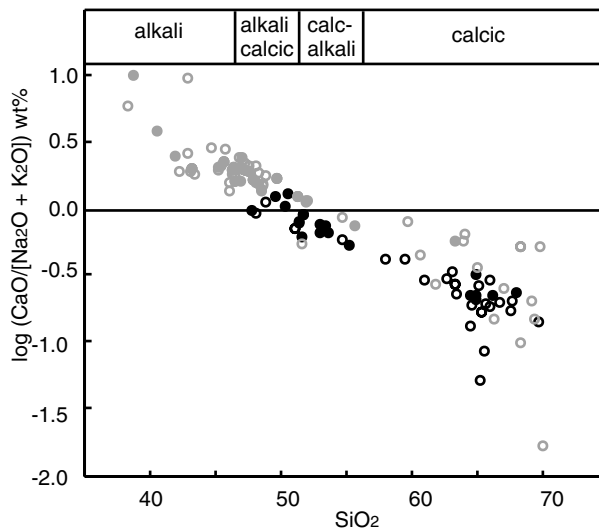


**Fig. 7.** Peacock Index Diagram for the ARC, MTZ, WFO, and SPS. Symbols and data sources as for Fig. 6.

and SPS (Fig. 8a–h). Subtle differences exist between all rock suites, but the data cluster into two groups of similar affinities; (i) ARC and MTZ samples; and (ii) WFO and SPS samples.

MTZ rocks range to considerably higher  $\text{SiO}_2$  contents than the ARC samples (up to 75 wt%); in most other respects, the suites are indistinguishable. Both fall along the same generalised fractionation path, through the gabbro-diorite-alkali granite fields (Fig. 6). Both fall in the middle of the calc-alkali field, with Peacock indices of 59 for the ARC and 58 for the MTZ (Fig. 7). For given  $\text{SiO}_2$  contents they show similar ranges and trends in major element abundances and both have very low Rb contents (Fig. 8a–g). Blattner & Williams (1991) reported that the Milford Gneiss and Darran Complex also have identical oxygen isotopic signatures, indicative of the same type of magma source, despite being significantly different from other calc-alkaline sequences. MTZ plutons have a primitive initial  $^{87}\text{Sr}/^{86}\text{Sr}$  of *c.* 0.70382 at 120 Ma (Muir *et al.*, 1998; Blattner & Graham, 2000), which is slightly higher than indicated by five analyses of the Milford Gneiss and Pembroke Granulite (Blattner & Graham, 2000).  $\epsilon_{\text{Nd}}$  values for the MTZ of *c.* +3 also record a primitive signature (McCulloch *et al.*, 1987; Muir *et al.*, 1998).

Though the WFO and SPS show a similar range in  $\text{SiO}_2$  contents, the SPS is dominated by silica-rich samples (*c.* 65–75 wt%), whereas the WFO is dominated by less silicic compositions (55–60 wt%). Both fall along a slightly more evolved fractionation path than the ARC-MTZ rocks, through the diorite/syenodiorite-alkali granite fields (Fig. 6). Both fall in the alkali-calcic range, with Peacock indices of 55 for the WFO and 54 for the SPS (Fig. 7). They show similar ranges and trends in major element abundances, which are

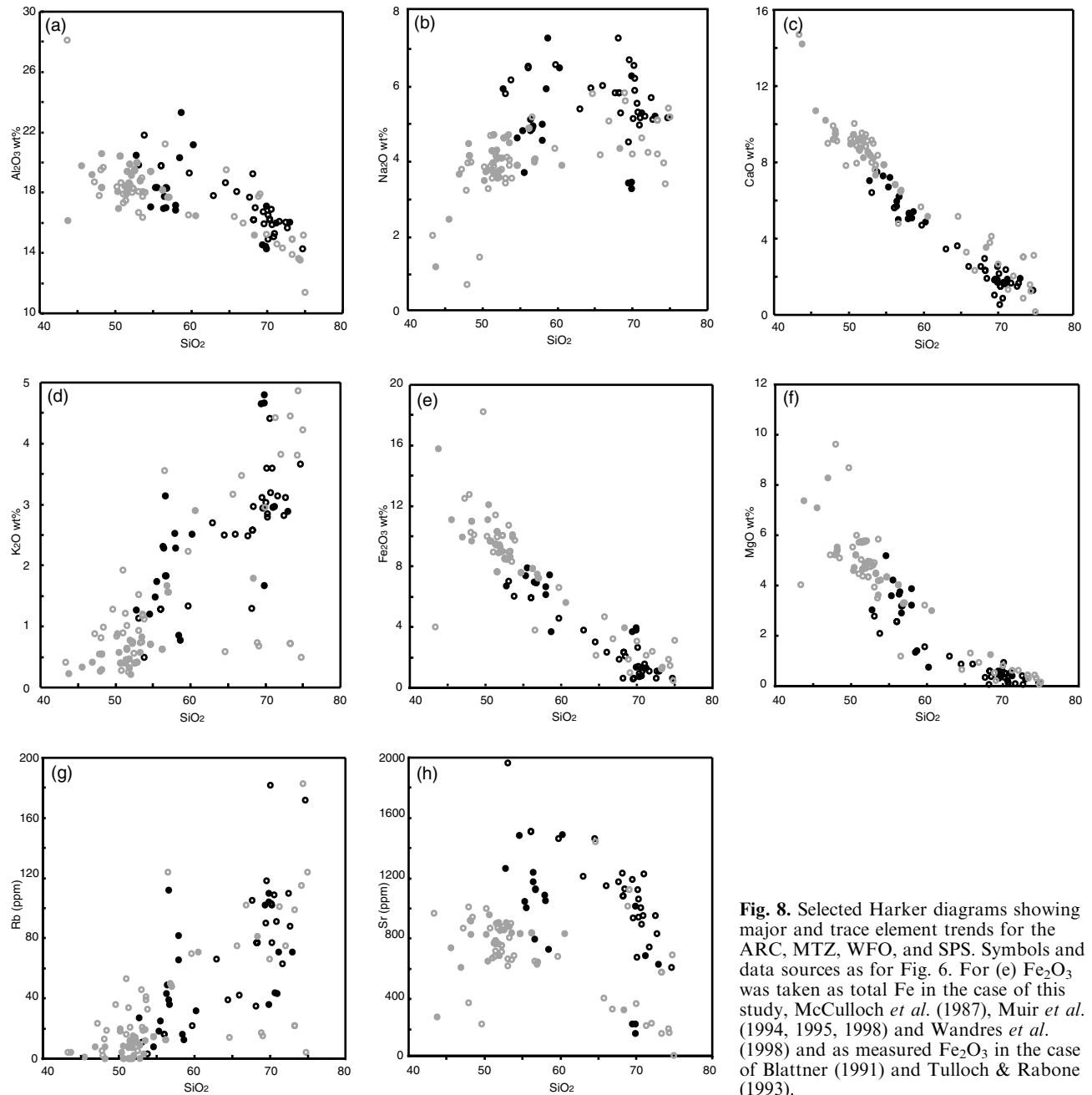


**Fig. 8.** Selected Harker diagrams showing major and trace element trends for the ARC, MTZ, WFO, and SPS. Symbols and data sources as for Fig. 6. For (e)  $\text{Fe}_2\text{O}_3$  was taken as total Fe in the case of this study, McCulloch *et al.* (1987), Muir *et al.* (1994, 1995, 1998) and Wandres *et al.* (1998) and as measured  $\text{Fe}_2\text{O}_3$  in the case of Blattner (1991) and Tulloch & Rabone (1993).

slightly different from the ARC-MTZ rocks: the WFO-SPS suite have higher  $\text{Na}_2\text{O}$  and  $\text{Al}_2\text{O}_3$  and lower  $\text{CaO}$  and  $\text{MgO}$  contents for given  $\text{SiO}_2$  contents. The WFO-SPS rocks also have high Rb and Sr abundances, with significantly higher Sr for given  $\text{SiO}_2$  content than the ARC-MTZ rocks (Fig. 8a–h). McCulloch *et al.* (1987) calculated an initial  $^{87}\text{Sr}/^{86}\text{Sr}$  of 0.70391 for the WFO and  $\epsilon_{\text{Nd}}$  values in the range  $-0.4$  to  $+2.7$  at 120 Ma. The SPS has a slightly higher initial  $^{87}\text{Sr}/^{86}\text{Sr}$  of  $0.70416 \pm 0.00002$  and consistent  $\epsilon_{\text{Nd}}$  values of  $+1.2$  to  $+1.8$  at 118 Ma (Muir *et al.*, 1995). Although relatively primitive, these values are

consistent with a slightly greater crustal component in the WFO-SPS relative to the ARC-MTZ rocks.

#### ZIRCON CHEMICAL AND MORPHOLOGICAL CONSTRAINTS ON AGE DATA

In order to place our geochronological data within a geological context we have addressed in some detail other constraints on the tectonic, magmatic and metamorphic history of Fiordland and the geochemical relationships between the important rock suites. Zircon chemistry, especially Th/U, can also be indicative of

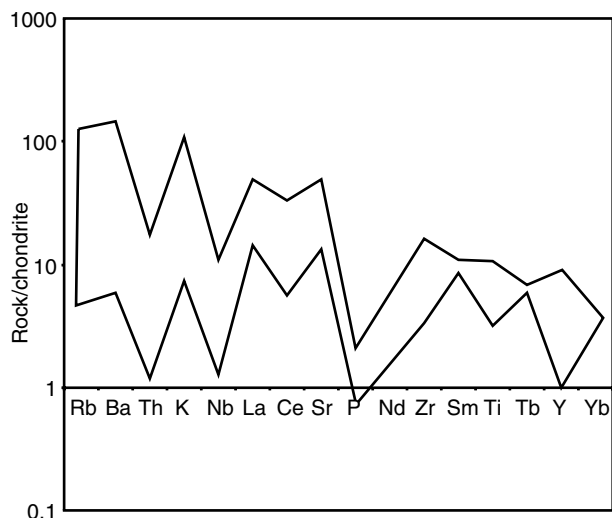


Fig. 9. Range in chondrite normalised REE abundances for 20 ARC samples from Mt Daniel, Mt Edgar, Milford Sound, Harrison Cove, and the Pembroke Valley. Data taken from this study and Blattner (1991).

particular geological settings (see Hoskin & Ireland, 2000), as can the morphology and internal crystallization structures (Vavra *et al.*, 1996), although these are not definitive and are subject to ongoing assessment. Nevertheless there are some specific features that can be used to support geological inferences. In this section we examine the relationships between zircon chemistry, morphology and age data in order to further constrain the magmatic and metamorphic history of Fiordland.

A zircon age range of 136–129 Ma for the ARC is interpreted as the range of emplacement ages for the magmatic protoliths. This interpretation is supported by the zircon chemistry and morphology. Zircon from ARC samples 9628 A, 9605, ME1, and 0224C have blocky grain shapes and, where present, poorly defined oscillatory zonation cut by sector zonation, moderate U contents (generally < 200 p.p.m) with comparatively high Th/U ratios (0.34–1.78). These features are typical of magmatic zircon from gabbroic rocks (Rubatto & Gebauer, 2000). This is supported by a  $133.4 \pm 2.1$  Ma emplacement age for the syn-post tectonic felsic dyke from Devil's Armchair (02DA), which cross-cuts the older Palaeozoic rocks in Camp Oven Creek. The euhedral strongly oscillatory-zoned zircon and large aspect ratios are typical of magmatic zircon from granitic rocks (Rubatto & Gebauer, 2000).

In comparison, metamorphic rims around magmatic and detrital cores usually have high U concentrations, and often extremely low Th/U-values (< 0.1). This supports a metamorphic origin for thin homogeneous Cretaceous rims on oscillatory-zoned zircon from the felsic dyke 02DA (U/Th = 0.01, 0.23) and from sample CO3 from Camp Oven Creek (U/Th = 0.00–0.05), and rims on homogeneous and sector-zoned cores

from SC2 from Selwyn Creek (*c.* 120 Ma, U/Th = 0.01–0.07).

Data from sample CO3 from Camp Oven Creek provides further support for a Cretaceous emplacement age for most of the ARC. Zircon from this sample has distinct morphological and chemical differences. The oscillatory-zoned cores are interpreted as having formed during the mid-Palaeozoic emplacement of the protolith, at  $346 \pm 6$  Ma, most probably associated with the Tuhua Orogeny. These analyses have significantly higher U than zircon from the other ARC samples (see Table S1). The presence of syn-D4 felsic segregations in this rock is consistent with the proposal that this is a mid-Palaeozoic enclave or an in-situ structure such as a pillar, which partially melted in the Cretaceous. It is unlikely that the Palaeozoic cores from CO3 could reflect the emplacement age of the ARC given the tight clustering of data and the scarcity of Palaeozoic zircon in the other five samples. Also, ME1 was collected from a relatively low-strain region, which shows no evidence for the intense D4 event evident at the other localities. Thus strain differences cannot be invoked as an argument for variable recrystallization of any inherited zircon components.

On the basis of their TIMS and SHRIMP U-Pb zircon study of a sample of the Milford Gneiss, Tulloch *et al.* (2000) concluded that the Arthur River Complex was Palaeozoic with substantial metamorphic overprint in the Cretaceous. The TIMS method yielded slightly discordant data with a lower intercept of  $136 \pm 15$  Ma and an upper intercept of  $364 \pm 34$  Ma. The SHRIMP method coupled with cathodoluminescence work resolved three zircon groups: (i) oscillatory zoned near-concordant  $355 \pm 10$  Ma cores (ii) large sector zoned near-concordant  $134 \pm 2$  Ma cores, and (iii) low-U, homogeneous  $120 \pm 2$  Ma rims on both Palaeozoic and Cretaceous cores. Tulloch *et al.* (2000) conceded that the tendency of TIMS results to plot more closely to the lower intercept and the proximity of similar aged plutons (e.g. the Darran Complex) support an Early Cretaceous emplacement with Palaeozoic inheritance. However, Palaeozoic emplacement of the ARC was favoured based on zircon morphological features: oscillatory zonation of Palaeozoic cores typical of igneous growth cf. sector zonation of Cretaceous cores interpreted as solid-state in origin. As indicated by Tulloch *et al.* (2000), the interpretation of the age of the Milford Gneiss is rather subjective because of the complex zircon systematics. However, the presence of minor Palaeozoic inheritance in only one of our samples and the tight clustering of data in all five indicates that the major event affecting the Milford Gneiss was at 136–129 Ma, and moreover this was a magmatic event. The Palaeozoic component is due to the variable presence of enclaves and inherited zircon assimilated into the Cretaceous magmas. The recognition of *c.* 120 Ma rims on older cores from both the Palaeozoic orthogneiss, CO3 ( $346 \pm 6$  Ma), and the

Cretaceous felsic dyke, 02DA ( $133.4 \pm 2.1$  Ma) support the existing evidence (Tulloch *et al.*, 2000) for a *c.* 120 Ma metamorphic event that affected the ARC coincident with the emplacement of the WFO.

Post-D4 pegmatite emplacement in the Pembroke Valley at  $81.8 \pm 1.8$  Ma was most likely associated with regional extensional tectonism at this time. The pegmatite was contemporary with A-type granites and mafic dykes in Westland-Nelson (*c.* 83 Ma; Muir *et al.* 1994;  $83 \pm 5$  Ma; Tulloch *et al.* 1991;  $81.7 \pm 1.8$  Ma – French Creek granite and Hohonu dyke swarm; Waight *et al.*, 1997) and the oldest oceanic crust in the Tasman Sea (*c.* 82 Ma; Weissel & Hayes, 1977). Inherited zircon material indicates significant mixing with early Cretaceous rocks with similar zircon morphologies and chemistries to those of the ARC and the WFO, and with Palaeozoic basement. This may have occurred via wall-rock interaction or contamination from the source of the pegmatite melt.

Dating of the dioritic gneiss from Selwyn Creek (SC2) has identified a distinct pluton, older than both the adjacent ARC and Darran Complex. For this reason we have assigned a new name: the Selwyn Gneiss. More work is required to constrain the position and nature of the boundaries between the Selwyn Gneiss, the ARC and the Darran Complex (Fig. 3). Zircon morphologies and chemical features in this sample are the same as the Cretaceous ARC host rock samples, and it has the same S4 fabric. On this basis, the age of  $154.4 \pm 3.6$  Ma is similarly interpreted as an emplacement age. This pluton may be equivalent to granites and monzonites of similar age (157–151 Ma), also on the western boundary of the MTZ at Lake Manapouri (Kimbrough *et al.*, 1994; Muir *et al.*, 1998) and with the *c.* 155 Ma dioritic Rotorua Complex in the same geological setting in Nelson (Kimbrough *et al.*, 1993, 1994). Cretaceous rims on zircon cores dated at *c.* 120 Ma rims are attributed to metamorphism associated with emplacement of the WFO.

#### IMPLICATIONS FOR THE CRETACEOUS EVOLUTION OF THE GONDWANA MARGIN

Emplacement of the ARC shortly before high-*P* metamorphism in a collisional tectonic setting is supported by metamorphic, structural and timing constraints. On the basis of cross-cutting relationships involving garnet reaction zones in the ARC in Milford Sound, Clarke *et al.* (2000) demonstrated that the ARC experienced early (D1) granulite facies conditions at  $P < 8$  kbar and  $T > 750$  °C, followed by high-*P* conditions (D2) of  $P \approx 14$  kbar and  $T > 750$  °C. Similar garnet reaction zones are observed in, and a similar *P*–*T* history inferred for, the 126–119 Ma WFO (Clarke *et al.*, 2000). Autometamorphism of a still hot ARC during collisional burial could account for the formation of D4 fabrics and assemblages in northern

Fiordland, more than 15 km distal from the WFO (see discussion of Clarke *et al.*, 2000). Accepting that mineral assemblages and structures in the WFO and ARC were synchronous, and that regional extension was underway by at least *c.* 110 Ma (J.D. Bradshaw, 1989; Kimbrough & Tulloch, 1989; Gibson & Ireland, 1995) this requires that the ARC was emplaced and buried to deep-crustal levels within approximately 20 Myr.

The predominance of younger plutons in the ARC (136–129 Ma) compared with the Darran Complex (143–136 Ma) precludes the possibility that these represent the same, but variably strained intrusive phase, as has been previously proposed on the basis of geochemical data (Blattner, 1991). However, the ARC and MTZ show very similar major element and trace element abundances and trends, consistent with their origin in the same evolving magmatic arc. Emplacement of the ARC as the youngest intrusive phase of the MTZ would be consistent with the observed trend toward younger magmatism in the western region of the MTZ (Kimbrough *et al.*, 1994). Given the presence of Palaeozoic orthogneiss (CO3) intruded by or entrained within the ARC, this requires that the ARC-MTZ and the Western Province had amalgamated by the time the ARC was emplaced.

The timing of emplacement of the ARC (136–129 Ma) shortly after the adjacent Darran Complex (143–137 Ma) and before the WFO (126–119 Ma) closes the gap between these two phases of magmatic activity. The timing, geological setting, and geochemical constraints are consistent with a continuum of magmatic activity within a setting that changed from island arc magmatism to arc-continent collision, rather than these representing distinct tectono-thermal events. The change in magma geochemistry from the calc-alkaline ARC-MTZ to the alkali-calcic, high alkali, high Sr WFO-SPS may be a significant indicator of these changed tectonic conditions in the early Cretaceous, shortly after emplacement of the ARC (e.g. Muir *et al.*, 1995, 1998). The WFO-SPS rocks preserve an ‘adakitic’ geochemical signature, involving  $\text{SiO}_2 > 56$  wt%, high alkalis, high  $\text{Al}_2\text{O}_3 (> 15$  wt%), high Sr ( $> 400$  p.p.m), low Y ( $< 18$ ), and high Sr/Y ( $> 20$ ). Adakites are arc rocks derived by melting of the subducting slab (Defant & Drummond, 1990) or of newly underplated basaltic crust (Atherton & Petford, 1993), rather than hydrous melting of the mantle wedge, as is normally the case for subduction-related magmas. The generation of adakitic WFO-SPS rocks has been discussed at length by Muir *et al.* (1995, 1998) who envisage that the change from calc-alkaline MTZ plutonism to the distinctive adakitic alkali-calcic WFO-SPS was tectonically triggered by thrusting of the MTZ beneath the continental Gondwana margin (the Western Province). This scenario is consistent with metamorphic and structural studies of the ARC (Clarke *et al.*, 2000; Daczko *et al.*, 2001a). Partial melting of an MTZ-sourced garnet-bearing

amphibolite in the deep crust is thought to have generated the Na, Sr and LREE enriched, and Y depleted WFO-SPS (Muir *et al.*, 1995, 1998).

The distribution and ages of terranes and U-Pb zircon age data for extensional magmatism in New Zealand and other regions thought to be contiguous in the Mesozoic indicate that by *c.* 105 Ma the tectonic regime in New Zealand had changed from convergence to extension (J. D. Bradshaw, 1989; Weaver *et al.*, 1994; Mukasa & Dalziel, 2000). The trigger for the onset of rifting shortly following emplacement of the WFO-SPS is the subject of some debate. J. D. Bradshaw (1989) proposed that the transition from convergence to extension was the result of ridge-trench collision. Luyendyk (1995) proposed a similar scenario, but instead of ridge-trench collision the trigger for the change was slab capture, in which the slab was too young and hot to be subducted, resulting in the ridge stalling outboard of the subduction zone. Given the very young age of the ARC and the evidence for high-*P* metamorphism in a collisional setting shortly after emplacement, this may have been achieved by subduction of these young hot plutons. The ensuing change in relative plate motions may have resulted in the onset of mid-Cretaceous extensional magmatism and the opening of the Tasman Sea.

## CONCLUSIONS

The ARC is formed from a Cretaceous batholith, emplaced along the palaeo-Pacific Gondwana margin at 136–129 Ma. We propose that the ARC represents the youngest phase of magmatism associated with the MTZ. This is based on (i) identical geochemistries of rocks of the ARC and MTZ and (ii) the timing of emplacement of the ARC with respect to MTZ magmatism. Intrusional relationships with a Palaeozoic enclave or wall rock ( $346 \pm 6$  Ma) indicate that the ARC was emplaced after amalgamation of the MTZ and the Western Province. This is supported by structural and metamorphic evidence for collisional burial of the ARC shortly after emplacement (e.g. Clarke *et al.*, 2000; Daczko *et al.*, 2001a). Thin rare rims on zircon cores from a Palaeozoic wall rock to the ARC, an ARC dyke, and the Selwyn Gneiss of the MTZ are all consistent with metamorphism of the rocks of Northern Fiordland at *c.* 120 Ma associated with emplacement of the WFO. An  $81.8 \pm 1.8$  Ma post-D4 pegmatite from the Pembroke Valley is correlated with extensional magmatism in Westland, and the opening of the Tasman Sea. The timing of emplacement of the ARC immediately following the last main phase of MTZ magmatism (157–131 Ma) and immediately prior to emplacement of the WFO-SPS suite (126–119 Ma and 124–111 Ma, respectively) is consistent with a continuum of Cretaceous magmatic activity that spanned the transition from island-arc magmatism to arc-continent collision.

## ACKNOWLEDGEMENTS

JAH, field and analytical work were supported by an Australian Research Council Grant to KAK and GLC (grant number A10009053) and National Science Foundation funding to KAK (EAR-0087323). NRD was supported by an Australian postgraduate award. J. Stevenson, J. Fitzhherbert, F. Schröter and M. Baker assisted in collecting SHRIMP analyses. J. Stevenson, B. Dockrill, A. Papadakis and J. Stevenson carried out some of the field work and some of the XRF and NAA analyses.

## REFERENCES

- Adams, C. J., 1987. Geochronology of granite terranes in the Ford Ranges, Marie Byrd Land, West Antarctica. *New Zealand Journal of Geology and Geophysics*, **30**, 51–72.
- Aronson, J. L., 1968. Regional geochronology of New Zealand. *Geochimica et Cosmochimica Acta*, **32**, 35–50.
- Atherton, M. P. & Petford, N., 1993. Generation of sodium-rich magmas from newly underplated basaltic crust. *Nature*, **362**, 144–146.
- Bishop, D. G., Bradshaw, J. D. & Landis, C. A., 1985. Provisional terrain map of South Island, New Zealand. In: *Tectonostratigraphic Terranes of the Circum-Pacific Region* (eds Howell, D. G., Jones, D. L., Cox, A. & Nur, A.), pp. 512–522. Circum-Pacific Council for Energy and Resources, Houston.
- Black, L. P., Kamo, S. L., Allen, C. M., Aleinikoff, J. N., Davis, D. W., Korsch, R. J. & Foudoulis, C., 2003. TEMORA 1: A quality zircon standard for Phanerozoic U-Pb geochronology. *Chemical Geology*, in press.
- Blattner, P., 1976. Replacement of hornblende by garnet in granulite facies assemblages near Milford Sound, New Zealand. *Contributions to Mineralogy and Petrology*, **55**, 181–191.
- Blattner, P., 1978. Geology of the crystalline basement between Milford Sound and Hollyford Valley, New Zealand. *New Zealand Journal of Geology and Geophysics*, **21**, 33–47.
- Blattner, P., 1991. North Fiordland transcurrent convergence. *New Zealand Journal of Geology and Geophysics*, **34**, 533–542.
- Blattner, P. & Graham, I. J., 2000. New Zealand's Darran Complex and Mackay Intrusives; Rb-Sr whole-rock isochrons in the Median Tectonic Zone. *American Journal of Science*, **300**, 603–629.
- Blattner, P. & Williams, J. G., 1991. The Largs high-latitude oxygen isotope anomaly (New Zealand) and climatic controls of oxygen isotopes in magma. *Earth and Planetary Science Letters*, **103**, 270–284.
- Borg, S. G., Stump, E., Chappell, B. W., *et al.*, 1987. Granitoids of northern Victoria Land, Antarctica; implications of chemical and isotopic variations to regional crustal structure and tectonics. *American Journal of Science*, **287**, 127–169.
- Bradshaw, J. D., 1989. Cretaceous geotectonic patterns in the New Zealand region. *Tectonics*, **8**, 803–820.
- Bradshaw, J. Y., 1985. Geology of the northern Franklin Mountains, northern Fiordland, New Zealand, with emphasis on the origin and evolution of Fiordland granulites. *PhD Thesis, University of Otago, Dunedin*.
- Bradshaw, J. D., 1993. A review of the Median Tectonic Zone: terrane boundaries and terrane amalgamation near the Median Tectonic Line. *New Zealand Journal of Geology and Geophysics*, **36**, 117–125.
- Bradshaw, J. Y., 1989a. Origin and metamorphic history of an Early Cretaceous polybaric granulite terrain, Fiordland, southwest New Zealand. *Contributions to Mineralogy and Petrology*, **103**, 346–360.

- Bradshaw, J. Y., 1989b. Early Cretaceous vein-related garnet granulite in Fiordland, southwest New Zealand: a case for infiltration of mantle-derived CO<sub>2</sub>-rich fluids. *Journal of Geology*, **97**, 697–717.
- Bradshaw, J. Y., 1990. Geology of crystalline rocks of northern Fiordland: details of the granulite facies Western Fiordland Orthogneiss and associated rocks. *New Zealand Journal of Geology and Geophysics*, **33**, 465–484.
- Bradshaw, J. Y., 1991. Mid-Palaeozoic age of granitoids in enclaves within Early Cretaceous granulites, Fiordland, southwest New Zealand. *New Zealand Journal of Geology and Geophysics*, **34**, 455–469.
- Bradshaw, J. Y., 1991. Zoned garnets in metapelites in western Fiordland, Southwest New Zealand; polychronic crystallisation and insight into the nature and extent of Early Cretaceous regional metamorphism. *New Zealand Journal of Geology and Geophysics*, **34/3**, 261–270.
- Brown, E. H., 1996. High-pressure metamorphism caused by magma loading in Fiordland, New Zealand. *Journal of Metamorphic Geology*, **14**, 441–452.
- Clarke, G. L., Klepeis, K. A. & Daczko, N. R., 2000. Cretaceous high-P granulites at Milford Sound, New Zealand: metamorphic history and emplacement in a convergent margin setting. *Journal of Metamorphic Geology*, **18**, 359–374.
- Cooper, R. A. & Tulloch, A. J., 1992. Early Palaeozoic terranes in New Zealand and their relationship to the Lachlan fold belt. *Tectonophysics*, **214**, 129–144.
- Daczko, N. R., Clarke, G. L. & Klepeis, K. A., 2001b. Transformation of two-pyroxene hornblende granulite to garnet granulite involving simultaneous melting and fracturing of the lower crust, Fiordland, New Zealand. *Journal of Metamorphic Geology*, **19**, 547–560.
- Daczko, N. R., Klepeis, K. A. & Clarke, G. L., 2001a. Evidence of Early Cretaceous collisional-style orogenesis in northern Fiordland, New Zealand and its effects on the evolution of the lower crust. *Journal of Structural Geology*, **23**, 693–713.
- Defant, M. J. & Drummond, M. S., 1990. Derivation of some modern arc magmas by melting of young subducted lithosphere. *Nature*, **347**, 662–665.
- Gibson, G. M., 1992. Medium-high-pressure metamorphic rocks of the Tuhua Orogen, western New Zealand, as lower crustal analogues of the Lachlan fold belt, SE Australia. *Tectonophysics*, **214**, 145–157.
- Gibson, G. M. & Ireland, T. R., 1995. Granulite formation during continental extension in Fiordland, New Zealand. *Nature*, **375**, 479–482.
- Gibson, G. M. & Ireland, T. R., 1999. Black Giants Anorthosite, New Zealand; a Palaeozoic analogue of Archean stratiform anorthosites and implications for the formation of Archean high-grade gneiss terranes. *Geology*, **27/2**, 131–134.
- Gibson, G. M., McDougall, I. & Ireland, T. R., 1988. Age constraints on metamorphism and the development of a metamorphic core complex in Fiordland, southern New Zealand. *Geology*, **16**, 405–408.
- Harrison, M. T. & McDougall, I., 1980. Investigations of an intrusive contact, Northwest Nelson, New Zealand; I, Thermal, chronological and isotopic constraints. *Geochimica et Cosmochimica Acta*, **44**, 1985–2004.
- Hoskin, P. W. O. & Ireland, T. R., 2000. Rare earth element chemistry of zircon and its use as a provenance indicator. *Geology*, **28**, 627–630.
- Ireland, T. R., 1992a. Origin of gneisses in the Charleston Metamorphic Group. In: *Geological Society of New Zealand and New Zealand Geophysical Society 1992 Joint Annual Conference*, (ed. Nobes, D. C.), **63A**, 83, Geological Society of New Zealand, Christchurch.
- Ireland, T. R., 1992b. Crustal evolution of New Zealand: evidence from age distributions of detrital zircons in Western Province paragneisses and Torlesse greywacke. *Geochimica et Cosmochimica Acta*, **56**, 911–920.
- Ireland, T. R. & Gibson, G. M., 1998. SHRIMP monazite and zircon geochronology of high-grade metamorphism in New Zealand. *Journal of Metamorphic Geology*, **16**, 149–167.
- Kimbrough, D. L., Mattinson, J. M., Coombs, D. S., Landis, C. A. & Johnston, M. R., 1992. Uranium-lead ages from the Dun Mountain ophiolite belt and Brook Street Terrane, South Island, New Zealand. *Geological Society of America Bulletin*, **104**, 429–443.
- Kimbrough, D. L. & Tulloch, A. J., 1989. Early Cretaceous age of orthogneiss from the Charleston Metamorphic Group, New Zealand. *Earth and Planetary Science Letters*, **95**, 130–140.
- Kimbrough, D. L., Tulloch, A. J., Coombs, D. S., Landis, C. A., Johnston, M. R. & Mattinson, J. L., 1994. Uranium-lead zircon ages from the Median Tectonic Zone, New Zealand. *New Zealand Journal of Geology and Geophysics*, **37**, 393–419.
- Kimbrough, D. L., Tulloch, A. J., Geary, E., Coombs, D. S. & Landis, C. A., 1993. Isotope ages from the Nelson region of South Island, New Zealand: structure and definition of the Median Tectonic Zone. *Tectonophysics*, **225**, 433–448.
- Klepeis, K. A., Clarke, G. L. & Rushmer, T., 2003. Magma transport and coupling between deformation and magmatism in the continental lithosphere. *GSA Today*, **13/1**, 4–11.
- Klepeis, K. A., Daczko, N. R. & Clarke, G. L., 1999. Kinematic vorticity and tectonic significance of superposed mylonites in a major lower crustal shear zone, northern Fiordland, New Zealand. *Journal of Structural Geology*, **21**, 1385–1405.
- Kretz, R., 1983. Symbols for rock-forming minerals. *American Mineralogist*, **68**, 277–279.
- Landis, C. A. & Coombs, D. S., 1967. Metamorphic belts and orogenesis in southern New Zealand. *Tectonophysics*, **4**, 501–518.
- LeMaitre, R. W., 1984. A proposal by the IUGS Subcommittee on the Systematics of Igneous Rocks for a chemical classification of volcanic rocks based on the total alkali silica (TAS) diagram. *Australian Journal of Earth Sciences*, **31**, 243–255.
- Luyendyk, B. P., 1995. Hypothesis for Cretaceous rifting of East Gondwana caused by subducted slab capture. *Geology*, **23**, 373–376.
- Mattinson, J. M., Kimbrough, D. L. & Bradshaw, J. Y., 1986. Western Fiordland Orthogneiss: Early Cretaceous arc magmatism and granulite facies metamorphism, New Zealand. *Contributions to Mineralogy and Petrology*, **92**, 383–392.
- McCulloch, M. T., Bradshaw, J. Y. & Taylor, S. R., 1987. Sm-Nd and Rb-Sr isotopic and geochemical systematics in Phanerozoic granulites from Fiordland, southwest New Zealand. *Contributions to Mineralogy and Petrology*, **97**, 183–195.
- Mortimer, N., Tulloch, A. J., Spark, R., *et al.*, 1999. Median batholith and Median Suite of New Zealand: new perspectives on the Phanerozoic igneous record of southern Gondwanaland. *African Journal of Earth Sciences*, **29**, 257–268.
- Muenker, C. & Cooper, R. A., 1995. The island arc setting of a New Zealand Cambrian volcano-sedimentary sequence; implications for the evolution of the SW Pacific Gondwana fragments. *Journal of Geology*, **103**, 687–700.
- Muir, R. J., Ireland, T. R., Weaver, S. D. & Bradshaw, J. D., 1994. Ion microprobe U-Pb zircon geochronology of granitic magmatism in the Western Province of the South Island, New Zealand. *Chemical Geology (Isotope Geoscience)*, **113**, 171–189.
- Muir, R. J., Ireland, T. R., Weaver, S. D., Bradshaw, J. D., Evans, J. A., Eby, G. N. & Shelley, D., 1998. Geochronology and geochemistry of a Mesozoic magmatic arc system, Fiordland, New Zealand. *Journal of the Geological Society of London*, **155**, 1037–1053.
- Muir, R. J., Weaver, S. D., Bradshaw, J. D., Eby, G. N. & Evans, J. A., 1995. The Cretaceous Separation Point batholith, New Zealand: granitoid magmas formed by melting of

- mafic lithosphere. *Journal of the Geological Society of London*, **152**, 689–701.
- Muir, R. J., Weaver, S. D., Bradshaw, J. D., Eby, G. N., Evans, J. A. & Ireland, T. R., 1996. Geochemistry of the Karamea Batholith, New Zealand, and comparisons with the Lachlan Fold Belt granites of SE Australia. *Lithos*, **39**, 1–20.
- Mukasa, S. B. & Dalziel, I. W. D., 2000. Marie Byrd Land, West Antarctica; evolution of Gondwana's Pacific margin constrained by zircon U-Pb geochronology and feldspar common-Pb isotopic compositions. *Geological Society of America Bulletin*, **112**, 611–627.
- Nathan, S., Thurlow, C., Warnes, P. & Zucchetto, R., 2000. *Geochronology Database for New Zealand Rocks*, 2nd edn. 1961–99. *Institute of Geological and Nuclear Sciences report 2000/11*, 51pp.
- Norrish, K. & Hutton, J. T., 1969. An accurate X-ray spectrographic method for the analysis of a wide range of geological samples. *Geochimica Cosmochimica Acta*, **33**, 431–453.
- Oliver, G. J. H., 1977. Feldspathic hornblende and garnet granulites and associated anorthosite pegmatites from Doubtful Sound, Fiordland, New Zealand. *Contributions to Mineralogy and Petrology*, **65**, 111–121.
- Pankhurst, R. J., Millar, I. L., Grunow, A. M. & Storey, B. C., 1993. The pre-Cenozoic magmatic history of the Thurston Island crustal block, West Antarctica. *Journal of Geophysical Research, B, Solid Earth and Planets*, **98**, 11835–11849.
- Raven, M. J. & Dickson, J. A. D., 1989. Fir-tree zoning: an indicator of pulsed crystallisation in calcite cement crystals. *Sedimentary Geology*, **65**, 249–259.
- Rubatto, D. & Gebauer, D., 2000. Use of cathodoluminescence for U-Pb zircon dating by ion microprobe; some examples from the Western Alps. In: *Cathodoluminescence in Geosciences* (eds Pagel, M., Barbin, V., Blanc, P. & Ohnenstetter, D.), pp. 373–400, Springer, Berlin.
- Sun, S. S., 1980. lead isotopic study of young volcanic rocks from mid-ocean ridges, ocean islands and island arcs. *Philosophical Transactions of the Royal Society of London*, **A297**, 409–445.
- Thompson, R. N., Morrison, M. A., Hendry, G. L. & Parry, S. J., 1984. An assessment of the relative roles of a crust and mantle in magma genesis: an elemental approach. *Philosophical Transactions of the Royal Society of London*, **A310**, 549–590.
- Tulloch, A. J., Ireland, T. R., Walker, N. W. & Kimbrough, D. L., 2000. U-Pb zircon ages from the Milford Orthogneiss, Milford Sound, northern Fiordland: Paleozoic igneous emplacement and Early Cretaceous metamorphism. *Institute of Geological and Nuclear Sciences Science Report*, **2000/6**, 23pp.
- Tulloch, A. J., Kimbrough, D. L. & Waight, T. E., 1991. The French Creek granite, North Westland, New Zealand – Late Cretaceous A-type plutonism on the Tasman Passive Margin. In: *Evolution of the Tasman Sea Basin* (eds van der Lingen, G. J., Swanson, K. M. & Muir, R. J.). *Proceedings of the Tasman Sea Conference, Christchurch, New Zealand*.
- Tulloch, A. J. & Rabone, S. D. C., 1993. Mo-bearing granodiorite porphyry plutons of the Early Cretaceous Separation Point Suite, West Nelson, New Zealand. *New Zealand Journal of Geology and Geophysics*, **36**, 401–408, A. A. Balkema, Rotterdam: New York.
- Vavra, G., Gebauer, D., Schmid, R. & Compston, W., 1996. Multiple zircon growth and recrystallization during polyphase Late Carboniferous to Triassic metamorphism in granulites of the Ivrea Zone (Southern Alps): an ion microprobe (SHRIMP) study. *Contributions to Mineralogy and Petrology*, **122**, 337–358.
- Waight, T. E., Weaver, S. D., Ireland, T. R., Maas, R., Muir, R. J. & Shelley, D., 1997. Field characteristics, petrography, and geochronology of the Hohonu Batholith and the adjacent Granite Hill Complex, North Westland, New Zealand. *New Zealand Journal of Geology and Geophysics*, **40**, 1–17.
- Wandres, A. M., Weaver, S. D., Shelley, D. & Bradshaw, J. D., 1998. Change from calc-alkaline to adakitic magmatism recorded in the Early Cretaceous Darran Complex, Fiordland, New Zealand. *New Zealand Journal of Geology and Geophysics*, **41**, 1–14.
- Weaver, S. D., Bradshaw, J. D. & Adams, C. J., 1991. Granitoids of the Ford Ranges, Marie Byrd Land, Antarctica. In: *Geological Evolution of Antarctica; Proceedings of the Fifth International Symposium on Antarctic Earth Sciences* (eds Thomson, M. R. A., Crame, J. A. & Thomson, J. W.), pp. 345–351, Cambridge University Press, Cambridge: New York.
- Weaver, S. D., Bradshaw, J. D. & Muir, R. J., 1994. Cretaceous magmatism in Marie Byrd Land and New Zealand; change from subduction to continental rifting. In: *Geological Society of New Zealand 1994 Annual Conference; Programme and Abstracts. Geological Society of New Zealand Miscellaneous Publication*, 80A. & 185pp.
- Weissel, J. K. & Hayes, D. E., 1977. Evolution of the Tasman Sea reappraised. *Earth and Planetary Science Letters*, **36**, 77–84.
- White, P. J., 1994. Thermobarometry of the Charleston metamorphic group and implications for the evolution of the Paparoa metamorphic core complex, New Zealand. *New Zealand Journal of Geology and Geophysics*, **37**, 201–209.
- Williams, I. S., Chappell, B. W., Chen, Y. D. & Crook, K. A. W., 1992. Inherited and detrital zircons; vital clues to the granite protoliths and early igneous history of southeastern Australia. In: *The Second Hutton Symposium on the Origin of Granites and Related Rocks; Proceedings*, (eds Brown, P. E. & Chappell, B. W.), pp. 272. Geological Society of America, Washington DC.
- Williams, J. G. & Harper, C. T., 1978. Age and status of the Mackay Intrusives in the Eglinton-Upper Hollyford area. *New Zealand Journal of Geology and Geophysics*, **21**, 733–742.
- Wood, B. L., 1972. Metamorphosed ultramafites and associated formations near Milford Sound, New Zealand. *New Zealand Journal of Geology and Geophysics*, **15**, 88–127.
- Wyszczanski, R. J., Gibson, G. M. & Ireland, T. R., 1997. Detrital zircon age patterns and provenance in late Paleozoic-early Mesozoic New Zealand terranes and development of the paleo-Pacific Gondwana margin. *Geology*, **25**, 939–942.

Received 20 June 2002; revision accepted 8 November 2002.